Non-Abelian Anyons in Periodically Driven Abelian Spin Liquids

Francesco Petiziol*
Technische Universität Berlin, Institut für Theoretische Physik, Hardenbergstraße 36, 10623 Berlin

(Received 28 February 2024; revised 26 April 2024; accepted 30 May 2024; published 17 July 2024)

We show that non-Abelian anyons can emerge from an Abelian topologically ordered system subject to local time-periodic driving. This is illustrated with the toric-code model, as the canonical representative of a broad class of Abelian topological spin liquids. The Abelian anyons in the toric code include fermionic and bosonic quasiparticle excitations which see each other as π fluxes; namely, they result in the accumulation of a π phase if wound around each other. Non-Abelian behavior emerges because the Floquet modulation can engineer a nontrivial band topology for the fermions, inducing their fractionalization into Floquet-Majorana modes bound to the bosons. The latter then develop non-Abelian character akin to vortices in topological superconductors, realizing Ising topological order. Our findings shed light on the non-equilibrium physics of driven topologically ordered quantum matter and may facilitate the observation of non-Abelian behavior in engineered quantum systems.

DOI: 10.1103/PhysRevLett.133.036601

Quasiparticles with anyon quantum statistics are predicted to appear as gapped excitations in topologically ordered (TO) quantum phases of matter, such as fractional quantum Hall and spin liquids [1,2]. Braiding anyons of Abelian type can change the many-body wave function by a phase factor. Braiding non-Abelian anyons, instead, can induce a unitary transformation in a topologically protected degenerate ground state, enabling fault-tolerant quantum computation [1,3,4]. Abelian anyons have been recently observed and manipulated in various engineered quantum systems, ranging from ultracold atoms in optical lattices [5,6] to Rydberg-atom arrays [7] and superconducting circuits [8,9], and first realizations of non-Abelian TO states have been reported in trapped ion quantum processors [10]. This progress motivates the study of TO phases out of equilibrium, such as subject to external control, which may both provide a stepping stone toward non-Abelian physics [4,9,11–13] and unveil novel effects, with examples being radical chiral Floquet phases [14,15] and fractionalized prethermalization [16].

Here we show that time-periodic driving can effectively turn an Abelian TO system into a non-Abelian one. We use as a testbed the paradigmatic toric-code model [3], which is believed to capture the fundamental low-energy physics of a large class of Abelian topological spin liquids [2,17] while remarkably being exactly soluble. This argues for the broad applicability of our results while enabling a clear illustration of the desired effect through exact methods. Abelian anyons in $\mathbb{Z}_2$ spin liquids like the toric code emerge as bosonic and fermionic quasiparticle excitations which see each other as π fluxes: Winding a fermion around a boson (and vice versa) results, unusually, in the accumulation of a π phase. We show that a local Floquet modulation can alter the picture by driving one anyon type, the fermion, into a superconducting phase with a nontrivial band topology. This induces the fractionalization of the fermions into pairs of Majorana modes which bind to the other anyon type (the boson), realizing non-Abelian Ising TO [1,4,18]. This is predicted through analytical high-frequency expansions and verified by numerical computation of the non-Abelian exchange phases. Our results shed light on the properties of driven interacting topological systems and promote the development of protocols to Floquet-engineer non-Abelian anyons [19,20] from Abelian phases, further motivated by the recent experimental realizations [7,8,21] and theoretical proposals [22–25] of toric-code TO in quantum simulators. Complementary to achievements in the manipulation of individual TO states [8–10], a Floquet-engineering approach has the appeal of realizing the background Hamiltonian, which stabilizes the desired TO states, makes anyons well-defined quasiparticles [26], and enables the study of dynamics.

The driven model.—The toric-code model [3,27] describes spin-1/2 systems on the bonds of a square $L \times L$ lattice [Fig. 1(a)] (L even hereafter) with Hamiltonian

$$\hat{H}_{\mathrm{tc}} = -\frac{g}{2}\sum_{v}\hat{A}_v - \frac{g}{2}\sum_{p}\hat{B}_p. \tag{1}$$

The labels p and v denote lattice plaquettes and vertices, g is a coupling constant, $\hat{A}_v = \prod_{i\in v}\hat{X}_i$ and $\hat{B}_p = \prod_{i\in p}\hat{Z}_i$ are four-spin interactions, and $\hat{X}_i, \hat{Y}_i, \hat{Z}_i$ are Pauli matrices for the ith spin. When convenient, we will also interpret $p = (p_x, p_y)$ and $v = (v_x, v_y)$ as coordinates of two separate plaquette and vertex lattices, respectively, both with lattice vectors $x = (1, 0)$ and $y = (0, 1)$. All four-spin operators in (1) commute with each other, making the

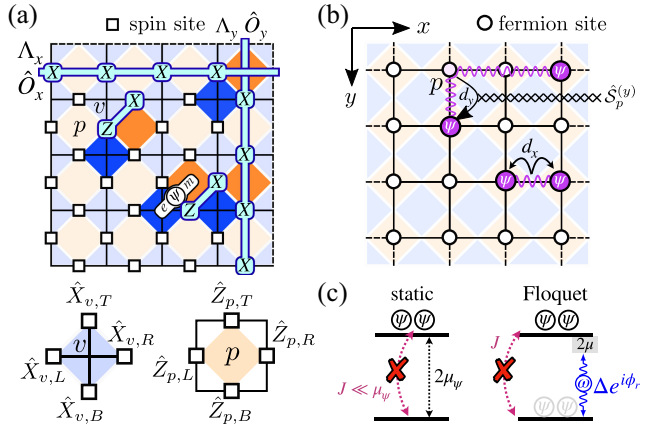

FIG. 1. (a) Toric-code spin lattice. The m anyons live on plaquettes p (orange), while e anyons live on vertices v (blue), and their bound state forms a fermion ψ. The operators $\hat{X}_i\hat{Z}_j$ depicted induce fermion tunneling and pairing. Dashed lines indicate periodic boundaries. (b) Corresponding lattice for ψ fermions in the quasiparticle mapping, where d_x and d_y control fermion tunneling and pairing. Vertical processes include a boson operator $\hat{\mathcal{S}}_p^{(y)}$ reproducing the mutual statistics of ψ and e. (c) Drive-assisted fermion pairing, restoring otherwise off resonant ($J \ll \mu_\psi$) processes with rate Δ and phase ϕ_r.

model exactly solvable. The eigenstates can be labeled by the eigenvalues $A_v = \pm 1$ and $B_p = \pm 1$ for each vertex and plaquette. On a torus, since $\prod_v \hat{A}_v = \prod_p \hat{B}_p = \mathbb{1}$, a complete set of observables is obtained by including two operators $\hat{O}_x = \prod_{i\in\Lambda_x}\hat{X}_i$ and $\hat{O}_y = \prod_{i\in\Lambda_y}\hat{X}_i$ spanning noncontractible loops [Λ_x and Λ_y in Fig. 1(a)] and commuting with all $\hat{A}_v$ and $\hat{B}_p$. The ± 1 eigenvalues of $\hat{O}_{x/y}$ define four superselection sectors, leading to four degenerate ground states satisfying $A_v = B_p = 1$. Flipping one eigenvalue, $A_v = -1$ ($B_p = -1$), costs an excitation energy g and is interpreted as the creation of a pointlike quasiparticle e (m) on top of the ground state $\mathbb{1}_{\mathrm{tc}}$, which occupies the corresponding vertex v (plaquette p). While e and m are hardcore bosons under self-exchange, they are mutual semions: The wave function picks up a Peierls-like π phase when m is wound around e, or vice versa. A bound state $\psi = e \times m$, costing an energy $\mu_\psi = 2g$, is then a fermion, while still being a semion with respect to a separate e or m. These quasiparticles, including $\mathbb{1}_{\mathrm{tc}}$, represent the four anyon types in the toric code. They are Abelian, since their nontrivial fusion has a single possible outcome: $e \times m = \psi$, $e \times \psi = m$, $m \times \psi = e$.

We add a drive to $\hat{H}_{\mathrm{tc}}$ to induce ψ-fermion motion and realize a topological band structure. Non-Abelian character will emerge from the interplay between the fermion band topology, achieved through Floquet engineering, and the semion relation between the ψ and e Abelian anyons, provided by the underlying toric code. The drive addresses neighboring spins as

$$\hat{H}_d(t) = -\sum_p [d_x(t)\hat{X}_{p,R}\hat{Z}_{p,B} + d_y(t)\hat{X}_{p,T}\hat{Z}_{p,L}]. \quad (2)$$

The subscripts (p, j), with $j \in \{B, R, T, L\}$ denote the spins at the bottom, right, top or left of p, respectively [Fig. 1(a)]. We expect drives of even simpler structure to achieve the desired effect, but (2) has the key merit that, while still being local, it allows for a transparent analytical treatment and efficient numerical simulation of the time-dependent system, as we shall see, thus enabling a clear illustration of the target physics. This is an important advantage: Investigating the toric code with even *static* magnetic-field perturbations generically requires sophisticated methods not directly applicable to the driven case [28–30]. Two-spin couplings of the form $\hat{X}_i\hat{Z}_j$ on adjacent spins induce ψ tunneling and pairing: They displace a pair of neighboring e and m composing ψ, as well as create and annihilate pairs of them. Indeed, since $\hat{X}_i$ anticommutes with $\hat{B}_p$ on neighboring plaquettes p and p' while commuting with $\hat{A}_v$, its action on an eigenstate flips the eigenvalues B_p and $B_{p'}$, while preserving the joint m-anyon parity $(-1)^{B_p+B_{p'}}$. Hence, if an m particle composing a fermion is present at p, it tunnels to p' (and vice versa). If no fermion or a pair is present, the associated pair of m will be created or annihilated. An equivalent analysis applies to e motion on nearby vertices induced by $\hat{Z}_j$. The functions $d_x(t)$ and $d_y(t)$ control processes along the horizontal and vertical direction, respectively.

Quasiparticle picture.—With the chosen form of the modulation, the driven model can be mapped exactly to a problem of driven noninteracting ψ fermions coupled to static e bosons, which allows us to focus on the impact of the drive on the ψ anyons. To this end, we adopt the quasiparticle picture of Ref. [31] (details are given in the Supplemental Material [32]). The spins' Hilbert space is mapped to the tensor product of Fock spaces for e hardcore-boson and ψ fermion occupations, and of a four-dimensional Hilbert space reflecting four superselection sectors. The spin operators map to creation and annihilation operators of bosons on vertices $(\hat{b}_v^\dagger, \hat{b}_v)$ and of fermions on plaquettes $(\hat{f}_p^\dagger, \hat{f}_p)$, with the toric-code ground state $|0_{\mathrm{tc}}\rangle$ representing the quasiparticle vacuum. The Hamiltonian $\hat{H}_{\mathrm{tc}}$ maps to $\hat{H}_e + \hat{H}_{e\psi}^{(0)}$ with $\hat{H}_e = g\sum_v \hat{b}_v^\dagger\hat{b}_v$ and $\hat{H}_{e\psi}^{(0)} = 2g\sum_p[1 - \hat{b}_{v(p)}^\dagger\hat{b}_{v(p)}]\hat{f}_p^\dagger\hat{f}_p$, describing quasiparticles at rest [$v(p)$ denotes the vertex to the bottom left of p]. The drive $\hat{H}_d(t)$ maps to $\hat{H}_{e\psi}^{(d)}(t) = -\sum_{p,r\in\{x,y\}} d_r(t)\hat{\mathcal{S}}_p^{(r)}(\hat{f}_p\hat{f}_{p+r} + \hat{f}_p^\dagger\hat{f}_{p+r} + \mathrm{H.c.})$, describing fermion tunneling and pairing but also containing a coupling to the e bosons through $\hat{\mathcal{S}}_p^{(x)} = 1$ and $\hat{\mathcal{S}}_p^{(y)} = \prod_{v\in\mathrm{R}[v(p)]}(-1)^{\hat{b}_v^\dagger\hat{b}_v}$. Here, $\mathrm{R}[v(p)]$ denotes the vertices to the right of the spin shared by the plaquettes p and $p + y$; see Fig. 1(b). This coupling explicitly reproduces the

semion mutual statistics: $\hat{\mathcal{S}}_p^{(r)}$ yields the accumulation of π phase when a fermion encircles an e particle. Since the drive does not induce boson motion, all bosonic terms are diagonal in the Fock basis $|\vec{n}^e\rangle = (\hat{b}_{v_1}^\dagger)^{n_1}\ldots(\hat{b}_{v_N}^\dagger)^{n_N}|0_{\rm tc}\rangle$ describing e occupations. We can then analyze the fermion Hamiltonian $\hat{H}_\psi(t) = \langle\vec{n}^e|\hat{H}_{e\psi}^{(0)} + \hat{H}_{e\psi}^{(d)}(t)|\vec{n}^e\rangle$ corresponding to a fixed distribution of e particles. The potential presence of e bosons at vertices $\{v\}$ is assumed to derive from preparing the ground state of a slightly modified Hamiltonian (1) with inverted coupling $g \to \tilde{g} = -g$ for those vertices. The Hamiltonian $\hat{H}_\psi(t)$ then reads as

$$\hat{H}_\psi(t) = \sum_p \Big[\mu_\psi \hat{f}_p^\dagger \hat{f}_p - \sum_{r\in\{x,y\}} d_r(t)\mathcal{S}_p^{(r)}(\hat{f}_p\hat{f}_{p+r} + \hat{f}_p^\dagger\hat{f}_{p+r} + \text{H.c.})\Big], \quad (3)$$

where $\mathcal{S}_p^{(r)} = \langle\vec{n}^e|\hat{\mathcal{S}}_p^{(r)}|\vec{n}^e\rangle$. It describes spinless superconducting fermions coupled, through $\hat{\mathcal{S}}_p^{(r)}$, to an effective gauge flux given by a background distribution of e particles. For a fixed e-boson distribution, the driven toric code then maps to a problem of driven *noninteracting* fermions.

Floquet engineering.—The above ingredients suggest a potential analogy to topological superconductors [1,38,39], where non-Abelian anyons emerge as vortices (σ) carrying Majorana zero modes [40]. The latter result from the fractionalization of the fermions occurring when their bulk bands are gapped and topological, as is the case for pairing in so-called $p+ip$ symmetry [1]. In the lattice model (3), this corresponds to a complex-valued pairing coupling $\Delta_r f_p^\dagger f_{p+r}^\dagger$ with $(\Delta_x, \Delta_y) = (\Delta, i\Delta)$ [17]. These so-called Ising anyons σ, $\mathbb{1}_{\rm is}$ and ψ feature nontrivial fusion rules $\sigma\times\sigma = \mathbb{1}_{\rm is} + \psi$, $\psi\times\psi = \mathbb{1}_{\rm is}$, $\psi\times\sigma = \sigma$ [1,4]. The multiple fusion channels for the vortex σ, yielding either the vacuum $\mathbb{1}_{\rm is}$ or a fermion ψ, qualify them as non-Abelian. We will show that the driven toric code reproduces faithfully this physics, with e particles behaving like σ vortices, for appropriate driving functions that Floquet-engineer complex fermion pairing.

Since the drive controls the physical spins, rather than the quasiparticle pairing terms directly, no choice of time-*in*dependent d_x and d_y in Eq. (2) can achieve the goal. Indeed, the functions $d_r(t)$ need be real valued, and they induce tunneling and pairing with equal real rate. We overcome these limitations employing a periodic modulation $d_r(t) = d_r(t+T)$ and Floquet engineering [41,42]. The driving functions are chosen as

$$d_r(t) = J + 2\Delta\cos(\omega t + \phi_r), \quad (4)$$

with frequency $\omega = 2\pi/T$ and amplitudes J and Δ much smaller than the fermion chemical potential, $J, \Delta \ll \mu_\psi$. They only differ in their phase ϕ_r. Consider first the limit $\Delta = 0$ in Eq. (4). Since the energy $2\mu_\psi$ required for pair creation and annihilation is much larger than J, pairing processes with a real coupling J in (3) are far off resonant and effectively suppressed, leaving only quasiparticle tunneling. They are restored via the modulation with $\Delta \neq 0$ and a frequency ω quasiresonant with $2\mu_\psi$ [Fig. 1(c)]. The advantage is that a complex phase can be attributed to the "photon-assisted" pairing coupling, depending on the phases ϕ_r of the drives. We choose $\omega = 2(\mu_\psi + \mu)$, allowing for a small detuning 2μ. Applying Floquet theory [43,44], the stroboscopic dynamics induced by the time-periodic Hamiltonian (3) in steps of T is captured as $\hat{U}(nT) = e^{-i\hat{H}_F nT}$ by a time-independent Floquet Hamiltonian $\hat{H}_F$, which can be approximated from $\hat{H}_\psi(t)$ through high-frequency expansions, in the regime $\omega \gg J, \Delta, \mu$ considered here [41,42,45–47]. To leading order in ω^{-1} and in a frame defined by $\hat{R}(t) = \exp[-it(\omega/2)\sum_p \hat{f}_p^\dagger\hat{f}_p]$ [32], $\hat{H}_F$ is approximated by the time-averaged Hamiltonian

$$\hat{H}_{\rm avg} = -\sum_p \Big[\mu\hat{f}_p^\dagger\hat{f}_p + \sum_{r=x,y}\mathcal{S}_p^{(r)}(\Delta e^{i\phi_r}\hat{f}_p\hat{f}_{p+r} + J\hat{f}_p^\dagger\hat{f}_{p+r} + \text{H.c.})\Big]. \quad (5)$$

At time T, $\hat{R}(T) = (-1)^{\sum_p \hat{f}_p^\dagger\hat{f}_p}$ reduces to the total fermion parity, which is a conserved quantity. Since quasiparticles in the toric code can only be created in pairs, only even-parity states are physical, and $\hat{R}(T) = 1$ in their subspace. The desired $p+ip$ pairing in $\hat{H}_{\rm avg}$ is obtained by choosing a circularlike shaking, with phase delay $\phi_y - \phi_x = \pi/2$ between horizontal and vertical modulations. The effective chemical potential μ is controlled by the detuning of the drive from the excitation energy of a fermion pair in the toric code, and the fermions are coupled to the e particles via $\mathcal{S}_p^{(r)}$.

Floquet-Majorana modes.—We verify that this Floquet modulation indeed induces topological properties and yields Floquet-Majorana modes. We study these properties by numerically computing the Floquet Bogoliubov-de Gennes (BdG) Hamiltonian $\hat{H}_{F,\rm BdG}$, defined by $\hat{H}_F = (1/2)(\hat{\boldsymbol{f}}^\dagger, \hat{\boldsymbol{f}})\hat{H}_{F,\rm BdG}(\hat{\boldsymbol{f}}, \hat{\boldsymbol{f}}^\dagger)^T$, as well as its quasienergy spectrum and ground state parity, from the driven model of Eq. (3) [32]. The topological phase is expected for $|\mu| < 4J$ and is characterized by a nonzero Chern number of the negative-energy fermion band [17,38,39]. Tuning the frequency ω to this topological region ($\mu \simeq -2J$), in the absence of e vortices [$\mathcal{S}_p^{(r)} = 1$], we find four nearly degenerate high-frequency "ground" states on a torus, one in each superselection sector corresponding to periodic

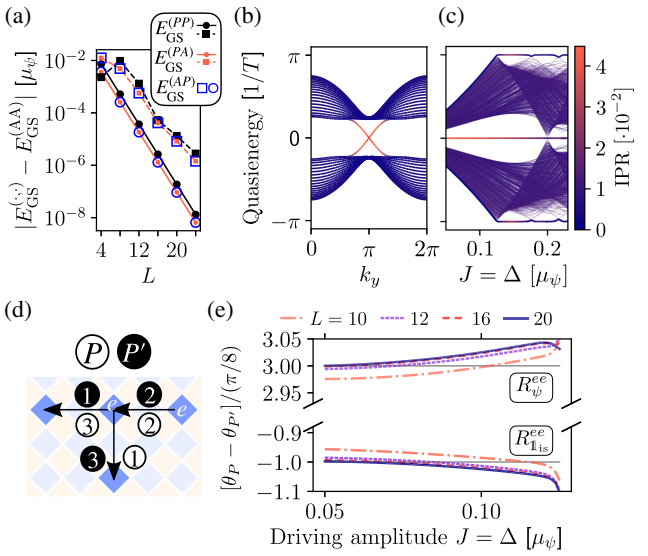

FIG. 2. (a) Splitting between fermion ground states for $\mu = -2J$ in different superselection sectors, having energy $E_{GS}^{(x,y)}$ [(x, y) denotes the boundary conditions, either periodic (P) or antiperiodic (A) along x and y] in the high-frequency regime ($J = \Delta = 0.1\mu_\psi$, solid lines and circles) and in the anomalous phase ($J = \Delta = 0.15\mu_\psi$, dashed lines and squares). (b) Floquet-BdG quasienergies on a $L_x \times L_y = 20 \times 200$ cylinder, for $J = \Delta = 0.1\mu_\psi$, and (c) on a (A, A) torus in the presence of an e pair, for increasing driving amplitude ($\mu = -2J$, $L = 24$). The color scale indicates the inverse participation ratio of the corresponding eigenstate. (d) Paths P and P' involved in the vortex-exchange protocol. (e) Vortex exchange phase $\theta_P - \theta_{P'}$ in the $\mathbb{1}_{is}$ (bottom) and ψ (top) sectors at $\omega = 2(\mu_\psi - 2J)$, for different driving amplitudes and system sizes.

or antiperiodic boundary conditions in x and y directions [38]. The topological degeneracy is approached exponentially with increasing system size, as shown in Fig. 2(a), and only three ground states have even fermion parity and are thus physical, signaling three Ising-anyon types $e, \mathbb{1}_{is}, \psi$. On a cylinder, the quasienergy spectrum exhibits two edge modes [Fig. 2(b)], indicating the development of nontrivial topology and a nonzero Chern number.

Introducing a pair of separated e particles on the torus, approximate Majorana modes at near-zero quasienergy appear [Fig. 2(c)], which persist until ω is detuned out of the topological phase, as predicted by the time-averaged description of Eq. (5). For weak driving the gap remains open as the amplitude $J = \Delta$ increases, indicating that higher-order terms neglected in (5) do not fundamentally alter the nature of the phase in this regime. Their impact can be suppressed exponentially with decreasing J/ω [48,49]. While generic periodically driven systems are expected to reach "infinite-temperature" at long times due to energy absorption from the drive [50,51], our model may evade such heating given that it maps to an integrable fermion system (and static bosons) [52,53]. We verify in the Supplemental Material [32] that this is indeed the case at high frequency, also for large e-particle densities. Increasing the driving amplitudes beyond the high-frequency regime, while maintaining $\mu = -2J$, the fermions enter an anomalous Floquet phase [42,54,55]. Here the time-averaged description of Eq. (5) is no longer valid, but the system still exhibits Majorana modes, at both quasienergy zero and $\pm\pi/T$; see Fig. 2(c). This effect, only possible in driven systems [54,56–63], has been proposed as a means to realize non-Abelian braiding and quantum computation in 1D Kitaev quantum wires [64–67].

Non-Abelian exchange phases.—We analyze whether the exchange statistics of two e particles (vortices) in the fermion topological phase is non-Abelian, as predicted in the presence of Majorana zero modes [4,40]. Two vortices are exchanged explicitly in different fusion sectors following Levin-Wen's protocol [4,68,69], sketched in Fig. 2(d), and Ref. [31]. The protocol computes the difference in the Berry phase accumulated by moving vortices along two paths P and P', sharing the same set of positions but involving a different order of vortex moves. This guarantees that the resulting phase is only determined by the exchange statistics [68]. For each intermediate vortex configuration $|\vec{n}_i^e\rangle$ along the paths, we numerically determine the corresponding even-parity ground state $|\Phi_i\rangle$ of the Floquet-BdG Hamiltonian [32]. The Berry phase accumulated along the path P is computed from the sequence of ground states as $\theta_P = \mathrm{Arg}\prod_{(i,i+1)\in P}\langle\Phi_{i+1}|\hat{Z}_{i+1,i}^f|\Phi_i\rangle$. Here, $\hat{Z}_{i+1,i}^f$ is the fermionic part of the quasiparticle representation of the spin operator $\hat{Z}_i$ which converts the vortex configuration $|\vec{n}_i^e\rangle$ into $|\vec{n}_{i+1}^e\rangle$ by displacing one e particle. Details about the evaluation of the matrix elements in θ_P are given in the Supplemental Material [32]. The prediction for Ising anyons is that the exchange phase $R_{\mathbb{1}_{is}}^{\sigma\sigma}$ in the $\mathbb{1}_{is}$ fusion sector (where the vortices fuse to the vacuum) and $R_\psi^{\sigma\sigma}$ in the ψ sector (where they fuse to a fermion ψ) differ by $\pi C/2$ for Chern number C, namely $R_{\mathbb{1}_{is}}^{\sigma\sigma} = e^{-i\pi C/8}$ and $R_\psi^{\sigma\sigma} = e^{3i\pi C/8}$ [4]—a signature of their non-Abelian nature [70]. The two sectors $\mathbb{1}_{is}$ and ψ are selected by creating the e pair on top of two different ground states, corresponding to doubly antiperiodic and doubly periodic fermion boundary conditions, respectively [31,71]. The counterclockwise exchange phases obtained are shown in Fig. 2(e), for varying driving amplitude in the high-frequency regime and for different system size. The results converge rapidly with the size toward the prediction for Ising TO with $C = 1$. We have thus shown that the e vortices carrying Floquet-Majorana modes, arising in the driven toric code in the high-frequency regime, behave like non-Abelian Ising anyons. The stability of the exchange phases for increasing driving amplitude in this regime confirms that higher-order corrections to the time-averaged Hamiltonian do not disrupt the topological phase, as anticipated. While the direct e exchange probed here is

a smoking-gun signature at zero temperature, fermion fractionalization can be detected at finite temperature, e.g., in the temperature dependence of Raman scattering intensities [72].

Conclusion.—We have shown that time-periodic driving of an Abelian-anyon system can induce non-Abelian topological order, using Kitaev's toric code as the paradigmatic example of a large class of Abelian topological phases. Our findings suggest a potential path toward non-Abelian anyons in synthetic quantum systems, where Abelian phases have been realized [7,8]. The model studied extends the range of potential candidates exhibiting 2D Floquet-Majorana physics beyond systems with intrinsic superconductivity or superfluidity [73,74] and offers a flexible playground where key parameters such as quasiparticle motion and pairing processes can be independently controlled via the drive. The toric code, known to be closely related to quantum dimer models [75–77], has been recently shown to describe dimer liquids of Rydberg excitations constrained by Rydberg blockade [78–80], where Abelian spin-liquid behavior has been observed [7]. This represents a promising setup to explore the ideas presented here, alongside adaptations of Floquet-engineering protocols for the toric code proposed in superconducting circuits [23,25].

The author is grateful to André Eckardt, Nathan Harshman, Alexander Schnell, Isaac Tesfaye, and Sandro Wimberger for helpful and inspiring discussions. The author also acknowledges funding from the Deutsche Forschungsgemeinschaft (DFG, German Research Foundation) via the Research Unit FOR 2414—Project No. 277974659.

*f.petiziol@tu-berlin.de

[1] C. Nayak, S. H. Simon, A. Stern, M. Freedman, and S. Das Sarma, Non-Abelian anyons and topological quantum computation, Rev. Mod. Phys. **80**, 1083 (2008).
[2] L. Savary and L. Balents, Quantum spin liquids: A review, Rep. Prog. Phys. **80**, 016502 (2017).
[3] A. Kitaev, Fault-tolerant quantum computation by anyons, Ann. Phys. (Amsterdam) **303**, 2 (2003).
[4] A. Kitaev, Anyons in an exactly solved model and beyond, Ann. Phys. (Amsterdam) **321**, 2 (2006).
[5] H.-N. Dai, B. Yang, A. Reingruber, H. Sun, X.-F. Xu, Y.-A. Chen, Z.-S. Yuan, and J.-W. Pan, Four-body ring-exchange interactions and anyonic statistics within a minimal toric-code Hamiltonian, Nat. Phys. **13**, 1195 (2017).
[6] J. Kwan, P. Segura, Y. Li, S. Kim, A. V. Gorshkov, A. Eckardt, B. Bakkali-Hassani, and M. Greiner, Realization of 1D anyons with arbitrary statistical phase, arXiv:2306.01737.
[7] G. Semeghini, H. Levine, A. Keesling, S. Ebadi, T. T. Wang, D. Bluvstein, R. Verresen, H. Pichler, M. Kalinowski, R. Samajdar, A. Omran, S. Sachdev, A. Vishwanath, M. Greiner, V. Vuletić, and M. D. Lukin, Probing topological spin liquids on a programmable quantum simulator, Science **374**, 1242 (2021).
[8] K. J. Satzinger, Y.-J. Liu, A. Smith, C. Knapp, M. Newman, C. Jones, Z. Chen, C. Quintana, X. Mi, A. Dunsworth, C. Gidney, I. Aleiner, F. Arute, K. Arya, J. Atalaya *et al.*, Realizing topologically ordered states on a quantum processor, Science **374**, 1237 (2021).
[9] Google Quantum AI and collaborators, Non-Abelian braiding of graph vertices in a superconducting processor, Nature (London) **618**, 264 (2023).
[10] M. Iqbal, N. Tantivasadakarn, R. Verresen, S. L. Campbell, J. M. Dreiling, C. Figgatt, J. P. Gaebler, J. Johansen, M. Mills, S. A. Moses, J. M. Pino, A. Ransford, M. Rowe, P. Siegfried, R. P. Stutz, M. Foss-Feig, A. Vishwanath, and H. Dreyer, Non-Abelian topological order and anyons on a trapped-ion processor, Nature (London) **626**, 505 (2024).
[11] H. Bombin, Topological order with a twist: Ising anyons from an Abelian model, Phys. Rev. Lett. **105**, 030403 (2010).
[12] J. R. Wootton, V. Lahtinen, Z. Wang, and J. K. Pachos, Non-Abelian statistics from an Abelian model, Phys. Rev. B **78**, 161102(R) (2008).
[13] H. Song, A. Prem, S.-J. Huang, and M. A. Martin-Delgado, Twisted fracton models in three dimensions, Phys. Rev. B **99**, 155118 (2019).
[14] H. C. Po, L. Fidkowski, T. Morimoto, A. C. Potter, and A. Vishwanath, Chiral Floquet phases of many-body localized bosons, Phys. Rev. X **6**, 041070 (2016).
[15] H. C. Po, L. Fidkowski, A. Vishwanath, and A. C. Potter, Radical chiral Floquet phases in a periodically driven Kitaev model and beyond, Phys. Rev. B **96**, 245116 (2017).
[16] H.-K. Jin, J. Knolle, and M. Knap, Fractionalized prethermalization in a driven quantum spin liquid, Phys. Rev. Lett. **130**, 226701 (2023).
[17] S. Sachdev, *Quantum Phases of Matter* (Cambridge University Press, Cambridge, England, 2023).
[18] G. Moore and N. Read, Non-Abelians in the fractional quantum Hall effect, Nucl. Phys. **B360**, 362 (1991).
[19] M. Kalinowski, N. Maskara, and M. D. Lukin, Non-Abelian Floquet spin liquids in a digital Rydberg simulator, Phys. Rev. X **13**, 031008 (2023).
[20] B.-Y. Sun, N. Goldman, M. Aidelsburger, and M. Bukov, Engineering and probing non-Abelian chiral spin liquids using periodically driven ultracold atoms, PRX Quantum **4**, 020329 (2023).
[21] D. Bluvstein, H. Levine, G. Semeghini, T. T. Wang, S. Ebadi, M. Kalinowski, A. Keesling, N. Maskara, H. Pichler, M. Greiner, V. Vuletić, and M. D. Lukin, A quantum processor based on coherent transport of entangled atom arrays, Nature (London) **604**, 451 (2022).
[22] H. Weimer, M. Müller, I. Lesanovsky, P. Zoller, and H. P. Büchler, A Rydberg quantum simulator, Nat. Phys. **6**, 382 (2010).
[23] M. Sameti, A. Potočnik, D. E. Browne, A. Wallraff, and M. J. Hartmann, Superconducting quantum simulator for topological order and the toric code, Phys. Rev. A **95**, 042330 (2017).

[24] R. Verresen, M. D. Lukin, and A. Vishwanath, Prediction of toric code topological order from Rydberg blockade, Phys. Rev. X **11**, 031005 (2021).
[25] F. Petiziol, S. Wimberger, A. Eckardt, and F. Mintert, Nonperturbative Floquet engineering of the toric-code Hamiltonian and its ground state, Phys. Rev. B **109**, 075126 (2024).
[26] L. Jiang, G. K. Brennen, A. V. Gorshkov, K. Hammerer, M. Hafezi, E. Demler, M. D. Lukin, and P. Zoller, Anyonic interferometry and protected memories in atomic spin lattices, Nat. Phys. **482–488**, 1195 (2008).
[27] X.-G. Wen, Quantum orders in an exact soluble model, Phys. Rev. Lett. **90**, 016803 (2003).
[28] S. Trebst, P. Werner, M. Troyer, K. Shtengel, and C. Nayak, Breakdown of a topological phase: Quantum phase transition in a loop gas model with tension, Phys. Rev. Lett. **98**, 070602 (2007).
[29] I. S. Tupitsyn, A. Kitaev, N. V. Prokof'ev, and P. C. E. Stamp, Topological multicritical point in the phase diagram of the toric code model and three-dimensional lattice gauge Higgs model, Phys. Rev. B **82**, 085114 (2010).
[30] S. Dusuel, M. Kamfor, R. Orús, K. P. Schmidt, and J. Vidal, Robustness of a perturbed topological phase, Phys. Rev. Lett. **106**, 107203 (2011).
[31] C. Chen, P. Rao, and I. Sodemann, Berry phases of vison transport in $\mathbb{Z}_2$ topologically ordered states from exact fermion-flux lattice dualities, Phys. Rev. Res. **4**, 043003 (2022).
[32] See Supplemental Material at http://link.aps.org/supplemental/10.1103/PhysRevLett.133.036601, which includes Refs. [33–37], where we discuss (i) the quasiparticle mapping, (ii) the high-frequency expansion yielding the Floquet Hamiltonian of Eq. (5), (iii) details about the computation of the ground states of the Floquet Bogoliubov-de Gennes Hamiltonian and of the vortex exchange phases, and (iv) an analysis of driving-induced heating.
[33] P. Ring and P. Schuck, *The Nuclear Many-Body Problem* (Springer-Verlag Berlin Heidelberg, Oxford, 1980).
[34] L. M. Robledo, Sign of the overlap of Hartree-Fock-Bogoliubov wave functions, Phys. Rev. C **79**, 1 (2009).
[35] A. Lazarides, A. Das, and R. Moessner, Equilibrium states of generic quantum systems subject to periodic driving, Phys. Rev. E **90**, 012110 (2014).
[36] T. Ishii, T. Kuwahara, T. Mori, and N. Hatano, Heating in integrable time-periodic systems, Phys. Rev. Lett. **120**, 220602 (2018).
[37] M. Heyl, P. Hauke, and P. Zoller, Quantum localization bounds Trotter errors in digital quantum simulation, Sci. Adv. **5**, eaau8342 (2019).
[38] N. Read and D. Green, Paired states of fermions in two dimensions with breaking of parity and time-reversal symmetries and the fractional quantum Hall effect, Phys. Rev. B **61**, 10267 (2000).
[39] M. Sato and Y. Ando, Topological superconductors: A review, Rep. Prog. Phys. **80**, 076501 (2017).
[40] D. A. Ivanov, Non-Abelian statistics of half-quantum vortices in p-wave superconductors, Phys. Rev. Lett. **86**, 268 (2001).
[41] M. Bukov, L. D'Alessio, and A. Polkovnikov, Universal high-frequency behavior of periodically driven systems: From dynamical stabilization to Floquet engineering, Adv. Phys. **64**, 139 (2015).
[42] A. Eckardt, Colloquium: Atomic quantum gases in periodically driven optical lattices, Rev. Mod. Phys. **89**, 011004 (2017).
[43] J. H. Shirley, Solution of the Schrödinger equation with a Hamiltonian periodic in time, Phys. Rev. **138**, B979 (1965).
[44] H. Sambe, Steady states and quasienergies of a quantum-mechanical system in an oscillating field, Phys. Rev. A **7**, 2203 (1973).
[45] N. Goldman and J. Dalibard, Periodically driven quantum systems: Effective Hamiltonians and engineered gauge fields, Phys. Rev. X **4**, 031027 (2014).
[46] A. Eckardt and E. Anisimovas, High-frequency approximation for periodically driven quantum systems from a Floquet-space perspective, New J. Phys. **17**, 093039 (2015).
[47] T. Mikami, S. Kitamura, K. Yasuda, N. Tsuji, T. Oka, and H. Aoki, Brillouin-Wigner theory for high-frequency expansion in periodically driven systems: Application to Floquet topological insulators, Phys. Rev. B **93**, 144307 (2016).
[48] D. A. Abanin, W. De Roeck, and F. m. c. Huveneers, Exponentially slow heating in periodically driven many-body systems, Phys. Rev. Lett. **115**, 256803 (2015).
[49] T. Mori, T. Kuwahara, and K. Saito, Rigorous bound on energy absorption and generic relaxation in periodically driven quantum systems, Phys. Rev. Lett. **116**, 120401 (2016).
[50] L. D'Alessio and M. Rigol, Long-time behavior of isolated periodically driven interacting lattice systems, Phys. Rev. X **4**, 041048 (2014).
[51] R. Moessner and S. L. Sondhi, Equilibration and order in quantum Floquet matter, Nat. Phys. **13**, 424 (2017).
[52] A. Russomanno, A. Silva, and G. E. Santoro, Periodic steady regime and interference in a periodically driven quantum system, Phys. Rev. Lett. **109**, 257201 (2012).
[53] A. Lazarides, A. Das, and R. Moessner, Periodic thermodynamics of isolated quantum systems, Phys. Rev. Lett. **112**, 150401 (2014).
[54] L. Jiang, T. Kitagawa, J. Alicea, A. R. Akhmerov, D. Pekker, G. Refael, J. I. Cirac, E. Demler, M. D. Lukin, and P. Zoller, Majorana fermions in equilibrium and in driven cold-atom quantum wires, Phys. Rev. Lett. **106**, 220402 (2011).
[55] M. S. Rudner, N. H. Lindner, E. Berg, and M. Levin, Anomalous edge states and the bulk-edge correspondence for periodically driven two-dimensional systems, Phys. Rev. X **3**, 031005 (2013).
[56] T. Oka and H. Aoki, Photovoltaic Hall effect in graphene, Phys. Rev. B **79**, 081406(R) (2009).
[57] T. Kitagawa, E. Berg, M. Rudner, and E. Demler, Topological characterization of periodically driven quantum systems, Phys. Rev. B **82**, 235114 (2010).
[58] D. E. Liu, A. Levchenko, and H. U. Baranger, Floquet Majorana fermions for topological qubits in superconducting devices and cold-atom systems, Phys. Rev. Lett. **111**, 047002 (2013).
[59] Q.-J. Tong, J.-H. An, J. Gong, H.-G. Luo, and C. H. Oh, Generating many Majorana modes via periodic driving: A superconductor model, Phys. Rev. B **87**, 201109(R) (2013).

[60] J. K. Asbóth, B. Tarasinski, and P. Delplace, Chiral symmetry and bulk-boundary correspondence in periodically driven one-dimensional systems, Phys. Rev. B **90**, 125143 (2014).
[61] M. Benito, A. Gómez-León, V. M. Bastidas, T. Brandes, and G. Platero, Floquet engineering of long-range p-wave superconductivity, Phys. Rev. B **90**, 205127 (2014).
[62] K. Wintersperger, C. Braun, F. N. Ünal, A. Eckardt, M. D. Liberto, N. Goldman, I. Bloch, and M. Aidelsburger, Realization of an anomalous Floquet topological system with ultracold atoms, Nat. Phys. **16**, 1058 (2020).
[63] M. Jangjan, L. E. F. Foa Torres, and M. V. Hosseini, Floquet topological phase transitions in a periodically quenched dimer, Phys. Rev. B **106**, 224306 (2022).
[64] R. W. Bomantara and J. Gong, Simulation of non-Abelian braiding in Majorana time crystals, Phys. Rev. Lett. **120**, 230405 (2018).
[65] R. W. Bomantara and J. Gong, Quantum computation via Floquet topological edge modes, Phys. Rev. B **98**, 165421 (2018).
[66] B. Bauer, T. Pereg-Barnea, T. Karzig, M.-T. Rieder, G. Refael, E. Berg, and Y. Oreg, Topologically protected braiding in a single wire using Floquet Majorana modes, Phys. Rev. B **100**, 041102(R) (2019).
[67] R. W. Bomantara and J. Gong, Measurement-only quantum computation with Floquet Majorana corner modes, Phys. Rev. B **101**, 085401 (2020).
[68] M. Levin and X.-G. Wen, Fermions, strings, and gauge fields in lattice spin models, Phys. Rev. B **67**, 245316 (2003).
[69] K. Kawagoe and M. Levin, Microscopic definitions of anyon data, Phys. Rev. B **101**, 115113 (2020).
[70] M. Cheng, V. Galitski, and S. Das Sarma, Nonadiabatic effects in the braiding of non-Abelian anyons in topological superconductors, Phys. Rev. B **84**, 104529 (2011).
[71] In the antiperiodic case, the even-parity ground state is the quasiparticle vacuum, such that the pair of vortices is created from and fuses to the vacuum. For the periodic case, the BdG ground state has odd parity and thus the physical even-parity ground state is the first-excited state containing one BdG fermion. The vortex pair thus fuses to this fermion.
[72] J. Nasu, J. Knolle, D. L. Kovrizhin, Y. Motome, and R. Moessner, Fermionic response from fractionalization in an insulating two-dimensional magnet, Nat. Phys. **12**, 912 (2016).
[73] X. Yang, B. Huang, and Z. Wang, Floquet topological superfluid and Majorana zero modes in two-dimensional periodically driven Fermi systems, Sci. Rep. **8**, 2243 (2018).
[74] R.-X. Zhang and S. Das Sarma, Anomalous Floquet chiral topological superconductivity in a topological insulator sandwich structure, Phys. Rev. Lett. **127**, 067001 (2021).
[75] G. Misguich, D. Serban, and V. Pasquier, Quantum dimer model on the kagome lattice: Solvable dimer-liquid and Ising gauge theory, Phys. Rev. Lett. **89**, 137202 (2002).
[76] O. Buerschaper, S. C. Morampudi, and F. Pollmann, Double semion phase in an exactly solvable quantum dimer model on the kagome lattice, Phys. Rev. B **90**, 195148 (2014).
[77] M. Iqbal, D. Poilblanc, and N. Schuch, Semionic resonating valence-bond states, Phys. Rev. B **90**, 115129 (2014).
[78] P. Tarabunga, F. Surace, R. Andreoni, A. Angelone, and M. Dalmonte, Gauge-theoretic origin of Rydberg quantum spin liquids, Phys. Rev. Lett. **129**, 195301 (2022).
[79] R. Verresen and A. Vishwanath, Unifying Kitaev magnets, kagomé dimer models, and ruby Rydberg spin liquids, Phys. Rev. X **12**, 041029 (2022).
[80] R. Samajdar, D. G. Joshi, Y. Teng, and S. Sachdev, Emergent $\mathbb{Z}_2$ gauge theories and topological excitations in Rydberg atom arrays, Phys. Rev. Lett. **130**, 043601 (2023).